

A contractor-renormalization study of Hubbard plaquette clusters

Shirit Baruch and Dror Orgad

Racah Institute of Physics, The Hebrew University, Jerusalem 91904, Israel

(Dated: November 4, 2010)

We implement the contractor-renormalization method to study the checkerboard Hubbard model on various finite-size clusters as function of the inter-plaquette hopping t' and the on-site repulsion U at low hole doping. We find that the pair-binding energy and the spin gap exhibit a pronounced maximum at intermediate values of t' and U , thus indicating that moderate inhomogeneity of the type considered here substantially enhances the formation of hole pairs. The rise of the pair-binding energy for $t' < t'_{\max}$ is kinetic-energy driven and reflects the strong resonating valence bond correlations in the ground state that facilitate the motion of bound pairs as compared to single holes. Conversely, as t' is increased beyond t'_{\max} antiferromagnetic magnons proliferate and reduce the potential energy of unpaired holes and with it the pairing strength. For the periodic clusters that we study the estimated phase ordering temperature at $t' = t'_{\max}$ is a factor of 2–6 smaller than the pairing temperature.

PACS numbers: 74.81.-g, 71.10.Fd

I. INTRODUCTION

It is by now generally accepted that spatial inhomogeneity may emerge either as a static or as a fluctuating effect in strongly-coupled models of the high-temperature superconductors, and indeed in many of the real materials.¹ What is far from being settled is the issue of whether such inhomogeneity is *essential* to the mechanism of high-temperature superconductivity from repulsive interactions. While most researchers would probably answer this question in the negative one should bare in mind the absence of a conclusive evidence that the single-band two-dimensional Hubbard model, widely believed to be the "standard model" of high-temperature superconductivity, actually supports superconductivity with a high transition temperature.² On the other hand, when examined on small clusters the same model and its strong-coupling descendent, the $t - J$ model, exhibit robust signs of incipient superconductivity in the form of a spin-gap and pair binding.¹ This fact points to the possibility that the strong susceptibility towards pairing is a consequence of the confining geometry itself.

This line of thought has been pursued in the past by considering the extreme limit where the electronic density modulation is so strong that the system consists of weakly coupled Hubbard ladders^{3,4} or plaquettes⁵. Beyond the questionable applicability of such models to the physical systems, which are at most only moderately modulated, it is clear that strong inhomogeneity, even if beneficial to pairing, is detrimental to the establishment of phase coherence and consequently to superconductivity. On both counts it is, therefore, desirable to extend the analysis to the regime of intermediate inhomogeneity.

Recently, the checkerboard Hubbard model, constructed from 4-site plaquettes with nearest-neighbor hopping t and on-site repulsion U , was studied as function of the inter-plaquette hopping t' (see Fig. 1). Tsai *et al.*⁶ diagonalized exactly the 4×4 site cluster (2×2

plaquettes) and found that the pair-binding energy, as defined by Eq. (2) below, exhibits a substantial maximum at $t' \approx t/2$ for $U \approx 8t$ and low hole concentration. Doluweera *et al.*⁷, on the other hand, used the dynamical cluster approximation in the range $0.8 \leq t'/t \leq 1$ and obtained a monotonic increase in both the strength of the d -wave pairing interaction and the superconducting transition temperature, T_c , towards a maximum that occurs in the homogeneous model.

In this paper, we use the contractor-renormalization (CORE) method⁸ to derive an effective low-energy Hamiltonian for the checkerboard Hubbard model, which we then diagonalize numerically on various finite-size clusters. We begin by establishing the region of applicability of the CORE approximation by contrasting its predictions with the exact results of Ref. 6 for 2×2 plaquettes. Our findings indicate that at low concentrations of doped holes the two approaches agree reasonably well unless t' is larger than a value, which increases with U . Deviations also appear for small t' when U is large. We identify probable sources of these discrepancies.

Based on the lessons gained from the small system we go on to study larger clusters of up to 10 plaquettes. These include the periodic 6×6 sites cluster and 2-leg and 4-leg ladders with periodic boundary conditions along their length. Within the region where CORE is expected to provide reliable results the pair-binding energy continues to exhibit a non-monotonic behavior with a pronounced maximum at intermediate values of t' and U . The precise location of the maximum depends on the cluster geometry but it typically occurs in the range $t'_{\max} \approx 0.5 - 0.7t$ and $U_{\max} \approx 5 - 8t$. The spin gap of the doped system follows a similar trend, often reaching the maximum slightly before the pair-binding energy. These findings demonstrate that moderate inhomogeneity, of the type considered here, can substantially enhance the binding of holes into pairs.

In an effort to elucidate the source of the maximum

we have looked into the content of the ground state and calculated the contributions of various couplings in the effective Hamiltonian to its energy. Our results indicate that for $t' < t'_{\max}$ the doped holes move in a background, which is composed predominantly of plaquettes that are in their half-filled ground state. This background possesses strong intra-plaquette singlet resonating valence bond (RVB) correlations, which facilitate the propagation of pairs relative to independent holes. The rise in the pair-binding energy while t' grows towards t'_{\max} is a result of a faster decrease of the pair kinetic energy in comparison to that of unpaired fermions. As t' crosses t'_{\max} and approaches the uniform limit the ground state contains a growing number of plaquettes that support antiferromagnetic (AFM) magnons. In this regime of increasing AFM correlations the kinetic energy changes relatively little with t' , and the decrease of the pair-binding energy for $t' > t'_{\max}$ is caused by the lowering of the energy of single holes due to their interactions with the magnons. Interestingly, we find that the maximum in the pair-binding energy of the periodic clusters is accompanied by a change in the crystal momentum of the single-hole ground state from the $\Gamma - M$ and symmetry related directions at $t' < t'_{\max}$ to the Brillouin-zone diagonals at $t' > t'_{\max}$. A similar correlation was also found for the 3-hole ground state of the 6×6 sites cluster.

While the pair-binding energy sets a pairing scale, T_p , a phase-ordering scale, T_θ , is provided by the phase stiffness. The latter was evaluated from the second derivative of the ground state energy with respect to a phase twist introduced by threading the system with an Aharonov-Bohm flux. We have found that as the twist is taken to zero, the CORE energy curvature typically converges towards a limiting value only when $t' < t'_{\max}$. Within this region the phase stiffness increases monotonically with t' . Our results indicate that for the lightly doped periodic clusters that we have considered phase fluctuations dominate over pairing, specifically, $T_p \approx 2 - 6T_\theta$ at $t' = t'_{\max}$. The limitations of the present study make it difficult to draw conclusions regarding the behavior of T_c in the two-dimensional thermodynamic limit.

We have also calculated the pair-field correlations between Cooper-pairs that reside on the most distant bonds allowed by our finite clusters. As expected, these correlations are consistent with d -wave pairing. However, in contrast to the pair-binding energy and the phase stiffness the correlations change little with t' and are small in magnitude. This discrepancy might be resolved in light of our finding that only few holes are tightly bound into pairs that reside within a single plaquette. Moreover, we obtain that the number of such pairs changes relatively little with t' with no apparent correlation to the substantial maximum in the pair-binding energy. Taken together these findings suggest that the correlation function which we and others often use to identify and quantify pairing in the Hubbard model may be ill-constructed to take account of the more extended and structured nature of pairing in this model.

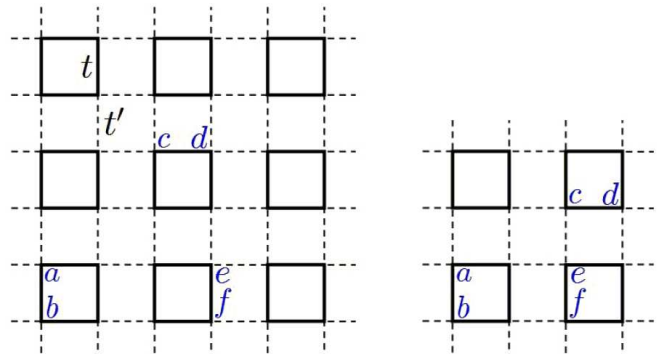


FIG. 1: The checkerboard Hubbard model. Shown here are two of the clusters that we studied. The bonds labeled ab , cd , and ef specify locations used in calculating the pairing correlations.

II. MODEL AND METHOD

The Hamiltonian of the checkerboard Hubbard model, which we have studied, is given by

$$H = - \sum_{\langle i,j \rangle, \sigma} (t_{ij} c_{i,\sigma}^\dagger c_{j,\sigma} + \text{H.c.}) + U \sum_i n_{i,\uparrow} n_{i,\downarrow}, \quad (1)$$

where $c_{i,\sigma}^\dagger$ creates an electron with spin $\sigma = \uparrow, \downarrow$ at site i of a two-dimensional square lattice. Here $n_{i,\sigma} = c_{i,\sigma}^\dagger c_{i,\sigma}$, and $\langle i,j \rangle$ denotes nearest-neighbor sites. The hopping amplitude is $t_{ij} = t$ for i and j on the same plaquette, while $t_{ij} = t'$ when they belong to neighboring plaquettes, as shown in Fig. 1.

The first step in obtaining the CORE effective Hamiltonian for the above model, is the exact diagonalization of a four-site plaquette. Out of the full spectrum, the M lowest-energy states are retained. The reduced Hilbert space, in which the effective Hamiltonian operates, is spanned by the tensor products of these states on different plaquettes. Next, the Hamiltonian (1) is diagonalized on N connected plaquettes and the M^N lowest-energy states are projected onto the reduced Hilbert space and Gram-Schmidt orthonormalized. Finally, after replacing the exact eigenstates by their projections, the N -plaquette Hamiltonian can be represented as one for M types of hard core particles coupled via N -body interactions. The CORE approximation consists of applying the resulting effective Hamiltonian to the study of larger clusters. By construction, the spectrum of the CORE Hamiltonian coincides with the low-energy spectrum of the exact problem on N plaquettes. We note, however, that this ceases to be the case if one or more of the exact low-energy states have zero projection on the reduced Hilbert space, or, if some of them are projected onto the same tensor-product state. In the following we demonstrate that such a problem arises in certain parameter regions of the model (1).

We concentrate on relatively low hole densities as measured from the half-filled system. The simplest trunca-

tion used to describe this regime is to retain the ground state of the half-filled plaquette [a total spin singlet $S = 0$ with plaquette momentum $\mathbf{q} = (0, 0)$], its $S = 1$, $\mathbf{q} = (\pi, \pi)$ triplet of lowest lying AFM magnon excitations, and the $S = 0$, $\mathbf{q} = (0, 0)$ hole pair ground state.⁹ The inclusion of the magnon excitations is essential for retrieving the correct magnetic behavior at low hole doping.¹⁰ Below we show that they also play an important role in the physics of hole binding. One can improve the approximation by including in the CORE plaquette basis also the two degenerate doublets $S_z = \pm 1/2$, $\mathbf{q} = (0, \pi), (\pi, 0)$, comprising the single hole ground state.^{10,11} Moreover, the inclusion of these states is mandatory for the purpose of calculating the pair binding energy, which is one of the goals of the present work. Consequently, our CORE scheme consists of keeping the above mentioned $M = 9$ states. We have considered only range-2 interactions, *i.e.* $N = 2$.

The resulting effective Hamiltonian includes all possible couplings, which respect the symmetries of the 2-plaquettes problem. These include the conservation of number of holes N_h , invariance under $SU(2)$ spin rotations and under reflections about the central bonds of the cluster in the x and y directions. The latter, together with the conservation of N_h , imply that within our reduced Hilbert space, as defined above, the total plaquette momentum $\mathbf{q}_1 + \mathbf{q}_2$ is also conserved (modulo 2π). We will not list here the 45 couplings which are allowed by the symmetries. Instead, we will describe the most important ones in the appropriate context and refer the reader to the Appendix for a detailed description of the Hamiltonian.

Many of the results reported in the following are derived from the spectrum of the effective Hamiltonian as obtained by exact diagonalization. We also calculate various ground-state correlations. To this end we project the appropriate operators on the reduced Hilbert space⁸ before evaluating their ground-state correlation function.

III. RESULTS

Although the size of the Hilbert space is massively reduced by the CORE approximation it still grows exponentially with the size of the system. Therefore, even the largest clusters that we are able to diagonalize using this method are too small for a direct calculation of T_c . Instead we calculate various properties of the system which are indicative of the two necessary ingredients for superconductivity: pairing and phase stiffness. We begin with the former and study its behavior as function of t' and U on various geometries. These include the 4×4 and 6×6 periodic clusters, seen in Fig. 1, as well as 2-leg and 4-leg ladders with periodic boundary conditions along their length, which extends up to 20 sites.

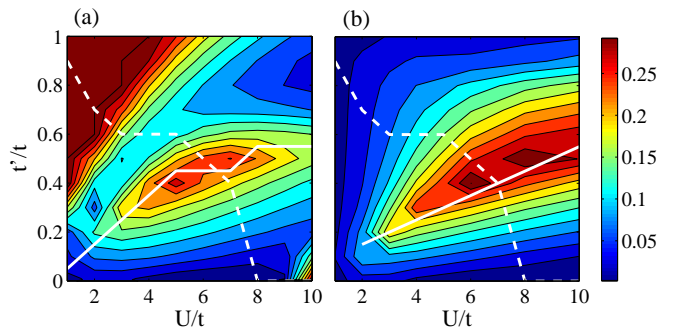


FIG. 2: The pair-binding energy in a periodic 4×4 cluster at $1/16$ hole doping as obtained by (a) CORE, and (b) exact diagonalization (Ref. 6). CORE projects out low energy states from the effective Hilbert space in the region above the dashed line. The crystal momentum of the degenerate single-hole ground state is $(0, \pi)$ and $(\pi, 0)$ below the solid line and $(0, 0)$ and (π, π) above it.

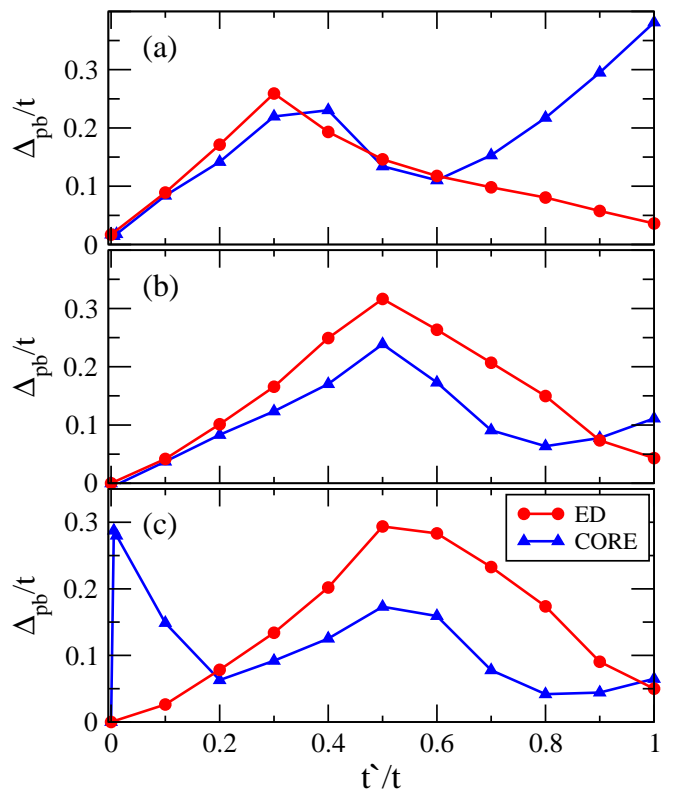


FIG. 3: The pair-binding energy in a periodic 4×4 cluster at $1/16$ doping for various values of the interaction strength (a) $U = 4t$, (b) $U = 8t$, and (c) $U = 10t$. Triangles depict the CORE results and circles correspond to the exact diagonalization results of Ref. 6.

A. Pair-binding energy and spin-gap

The pair-binding energy is defined by

$$\Delta_{pb}(M/N) = 2E_0(M) - [E_0(M+1) + E_0(M-1)], \quad (2)$$

where $E_0(M)$ is the ground-state energy of the system with M holes doped into the N -site half-filled cluster. Consider two identical clusters each with M holes. If holes tend to pair and M is odd it should be energetically favorable to move an electron from one cluster to another in order to obtain a fully-paired state in both. On the other hand, such a redistribution should be unfavorable if M is even. In this sense, a positive Δ_{pb} for odd M and a negative Δ_{pb} for even M signifies an effective attraction between holes.

Recently, Tsai *et al.*⁶ have found by exact diagonalization of the periodic 4×4 cluster that the pair-binding energy exhibits a pronounced maximum both as function of t' and U . Their results allow for a critical evaluation of the validity of the CORE method in a range of parameters. To this end we present in Figs. 2 and 3 a comparison between the CORE and the exact results for $\Delta_{pb}(1/16)$. It is clear that CORE introduces substantial errors in two specific regimes: small U and large t' [Fig. 3(a)], and large U and small t' [Fig. 3(c)], while it is in reasonable agreement with the exact results in the intermediate parameter regime.

An obvious source for the discrepancies is the fact that our CORE approximation includes only range-2 couplings. Longer-range interactions are expected to become more important as the system becomes more homogeneous *i.e.* when $t' \rightarrow t$. We believe that the deviations between the CORE predictions and the exact results in this limit, especially for small U where the pair size is expected to be large, are mainly due to insufficient range of the effective interactions. A related problem may emerge at large U where the extent of magnetic correlations grow. However, we did not confirm these conjectures by explicit calculations.

A more subtle source of errors, which we have mentioned already in the previous Section, is the fact that low-energy states may be projected out from the CORE effective Hilbert space in the process of generating the effective Hamiltonian. This happens when a low-lying state of a connected cluster has zero overlap with the tensor-product states of the effective Hilbert space or when two or more low-lying states are mapped onto the same state in the effective space (Note, however, that spin-rotation symmetry is preserved in the sense that spin multiplets are either kept or projected out as a whole.) Fig. 4 depicts for each of the sectors in which such a problem arises the excitation energy of the lowest projected-out state in units of the bandwidth of the kept states in the sector. We also denoted in Figs. 2 and 5 the parameter region where the problem occurs.

The overlap issue is responsible for the failure of CORE in the regime of small t' and large U . When $U > 7.858t$ and for $t' = 0$ the $N_h = 1, S = 3/2$ double-plaquette (eight-fold degenerate) ground state $|N_h = 1, S = 3/2\rangle_2$ consists of one plaquette in its half-filled ground state and a second plaquette in a fully-polarized $S = 3/2$ single-hole state. The latter resides outside the effective Hilbert space and therefore $|N_h = 1, S = 3/2\rangle_2$ is projected out.

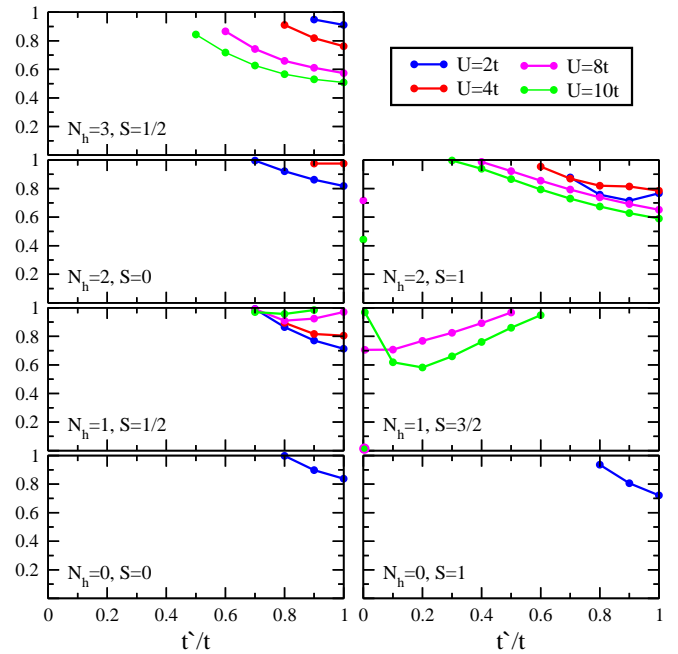


FIG. 4: The excitation energy of the lowest energy state that is projected-out by CORE in units of the bandwidth of the kept states in its sector.

This ceases to be the case once t' is turned on as a result of a component which appears in $|N_h = 1, S = 3/2\rangle_2$ and corresponds to a system with a magnon on one plaquette and a plaquette-fermion on the other. However, the amplitude of this component diminishes with increasing U . This leads CORE to misidentify the nature of $|N_h = 1, S = 3/2\rangle_2$ and induces an abrupt increase in the magnon-fermion interaction $[V_{ft}^{3/2,\nu,\mathbf{q}}$ in Eq. (A5)] for small t' . As a result, CORE underestimates the energy of the two-hole ground state of the 4×4 cluster and consequently predicts an erroneously large pair-binding energy, see Fig. 3. Nevertheless, it appears that away from this region of parameters the projected-out states are high enough in energy as to not cause qualitative errors.

Based on the comparison of Δ_{pb} depicted in Figs. 2,3 and similar plots presented below for the spin-gap [Fig. 6(a)] and pair-field correlations [Fig. 13(a)] we conclude that CORE agrees semi-quantitatively with the exact results provided $U/50 \lesssim t' \lesssim U/8$. Within this region, and across all geometries studied, we found the pair-binding energy to exhibit the same qualitative behavior consisting of a broad peak both as function of t' and U . This conclusion holds true also when one varies the doping level (at least in the low-doping regime which we have considered) as can be seen from the results for the 6×6 cluster presented in Fig. 5. In addition, the same figure suggests that the above mentioned problems with the CORE method become less severe as the size of the system increases.

The association of positive pair-binding energy with

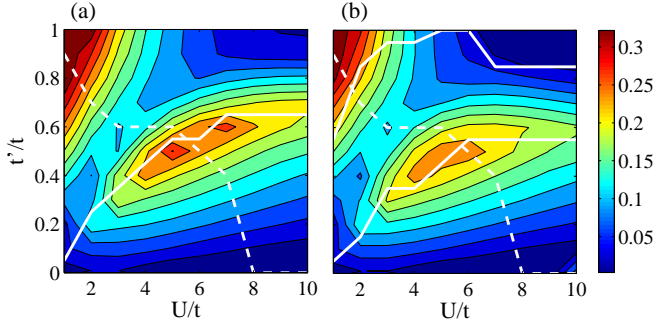


FIG. 5: The pair-binding energy in a periodic 6×6 cluster at (a) $1/36$, and (b) $3/36$ hole doping. CORE projects out low energy states from the effective Hilbert space in the region above the dashed line. In (a) the crystal momentum of the degenerate single-hole ground state is $(0, \pm 2\pi/3)$ and $(\pm 2\pi/3, 0)$ below the solid line and $(\pm 2\pi/3, \pm 2\pi/3)$ above it. In (b) the crystal momentum of the degenerate 3-hole ground state is $(\pm 2\pi/3, \pm 2\pi/3)$ between the solid lines and $(0, \pm 2\pi/3)$ and $(\pm 2\pi/3, 0)$ elsewhere.

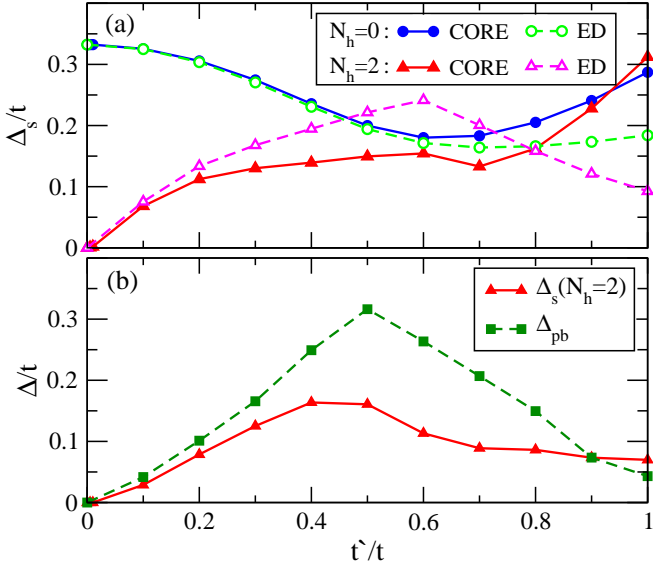


FIG. 6: The spin gap of undoped and two-hole doped systems at $U = 8t$. (a) The 4×4 periodic cluster - comparison between CORE and exact diagonalization results. (b) CORE results for the spin-gap Δ_s and the pair-binding energy $\Delta_{pb}(1/36)$ of the 6×6 periodic cluster.

Cooper pairing may be contested on the ground that it can also be taken as evidence for a tendency of the system to phase separate. We believe that this is not the case for the model studied here for the following reasons. First, in accordance with the interpretation discussed above of Δ_{pb} as indication for hole pairing we have found its sign to change according to $(-1)^{M+1}$ for all the clusters and doping levels which we have considered. Second, while the appropriate criteria for identifying regimes of phase separation from finite size studies include the Maxwell construction¹² and measurements of the sur-

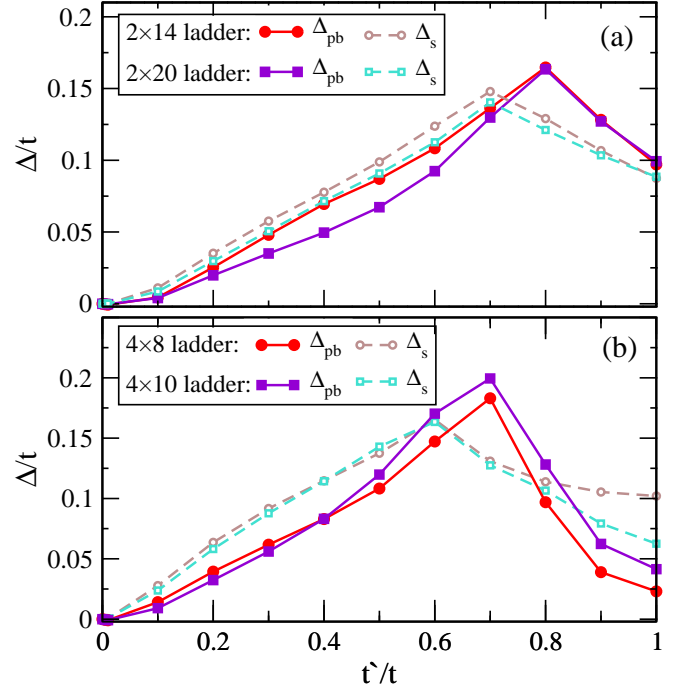


FIG. 7: The spin-gap Δ_s and pair-binding energy Δ_{pb} at $U = 8t$ for two-hole doped a) 2-leg ladders, (b) 4-leg ladders.

face tension in the presence of boundary conditions that force phase coexistence, a crude way of identifying phase separation is by calculating the inverse compressibility $\kappa^{-1} = n^2 \partial \mu / \partial n$, where μ is the chemical potential and n the electronic density. For numerical purposes a discrete version is used, which in our case reads

$$\kappa^{-1} \propto E_0(M+2) + E_0(M-2) - 2E_0(M). \quad (3)$$

Negative inverse compressibility indicates instability towards phase separation. We always find $\kappa^{-1} > 0$. Finally, whenever the ground state is a spin singlet one can define the spin-gap as the energy gap to the lowest $S = 1$ excitation. We have calculated the spin gap for the two-hole doped systems and found that in all cases it follows the pair-binding energy in the regime of small to moderate t' , see Figs. 6 and 7. This coincidence strongly suggests that in this regime the lowest $S = 1$ excitation is a result of a dissociation of a hole pair into two separate holes. It is interesting to note that we always observe that the spin-gap reaches a maximum and starts to drop before the pair-binding energy does so. This may be an indication that moderate inhomogeneity supports the formation of a bound $S = 1$ magnon-hole-pair state.^{10,13}

Consequently, our findings and the above arguments lead us to conclude that inhomogeneity of the type included in the checkerboard Hubbard model substantially enhances hole-pairing. The precise position of the point of optimal inhomogeneity in the sense of strongest pairing depends on the cluster geometry and interaction strength. Albeit, it typically occurs in the range $t'_{\max} \approx 0.5-0.7t$ and $U_{\max} \approx 5-8t$. We note that this fact

implies that the physics behind the large pairing scale of the model necessarily involves inter-plaquette couplings since the single plaquette does not support hole-pairing beyond $U_c \approx 4.6t$.⁹

B. Energetics and structure of the ground state

What drives the enhancement of hole-pairing and what is the reason for its maximum as function of t' ? In an attempt to gain insights into these questions we have took advantage of the fact that CORE provides us with an effective Hamiltonian whose various couplings can be classified and analyzed. To this end we have divided the 45 different couplings into four groups, as described in the Appendix. They include: fermion and hole-pair "bare" kinetic terms (including fermion and pair hopping as well as Andreev-like pair creation and disintegration), magnon-assisted fermion and pair hopping, fermion and pair interactions and finally, interactions involving magnons. Fig. 8 depicts the contribution of each group to the ground-state energy of the $N_h = 0, 1, 2$ doped 6×6 periodic cluster and to its pair-binding energy $\Delta_{pb}(1/36)$ at $U = 8t$.

Fig. 8 makes it clear that the increase in the pair-binding energy from $t' = 0$ to t'_{\max} is dominated by a faster decrease of the kinetic energy of hole pairs as compared to unpaired holes. Furthermore, in this region the pair-binding energy is largely determined by the "bare" kinetic terms while the (negative) contribution of hopping processes that involve magnons is much smaller. The small contributions of the various interactions approximately cancel out. Looking more closely at the way charges propagate in this range of t' we found that the main channel for single holes is a direct hop between neighboring plaquettes but that this process is virtually non-existent for hole pairs. Instead, a pair propagates predominantly by Andreev-like dissociation into single holes on adjacent plaquettes and recombination of these holes into a pair one register away from its original position [as described by the last term in Eq. (A2)].

For $t' > t'_{\max}$ the behavior changes qualitatively and rather abruptly. The gain in kinetic energy of the pair relative to that of unpaired holes ceases to increase. While pairs continue to propagate mainly via a series of dissociation and recombination events, single holes move almost exclusively by hopping processes involving magnons [the second and third terms in Eq. (A3)]. The decrease in the pair-binding energy in this regime is induced by a sharp decrease of the potential energy of the unpaired holes owing to their interactions with the magnons. On the other hand, the contribution of interactions not involving the magnons to the pair-binding energy does not show a significant change as t' is driven through t'_{\max} .

The above results suggest that the AFM magnons play an important role in inducing the change in the behavior of the pair-binding energy. To further test this conclusion we have looked at the evolution of the ground-

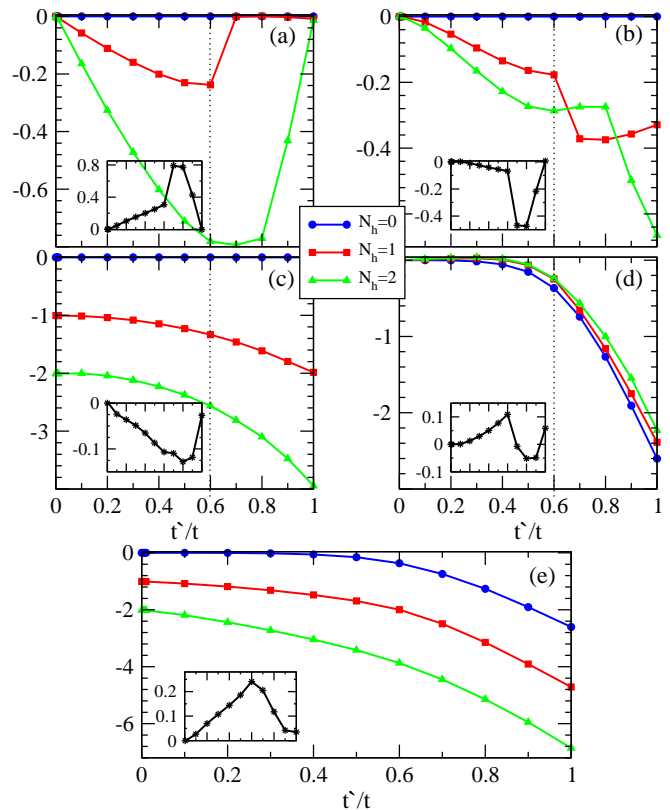


FIG. 8: Ground state expectation values of various effective couplings for the 6×6 periodic cluster at $U = 8t$: (a) fermion and pair hopping; (b) fermion and pair magnon-assisted hopping; (c) fermion and pair interactions; (d) interactions involving magnons; (e) the full Hamiltonian. The insets show the contribution of each group of couplings to the pair-binding energy. The full binding energy reaches a maximum at $t' = 0.6t$ as indicated by the dotted line.

state content with t' . Fig. 9 shows the average number of magnons, fermions and pairs in the $N_h = 0 - 4$ ground states of the 6×6 periodic cluster. Evidently, the magnons begin to proliferate slightly before the maximum in the pair-binding energy is reached. Concomitantly, there is an increase of AFM correlations in the system as can be seen from Fig. 10, which depicts the staggered magnetization $m_{(\pi,\pi)}$ defined by

$$m_{(\pi,\pi)}^2 = \left\langle \left[\frac{1}{N} \sum_{j=1}^N e^{i\mathbf{Q} \cdot \mathbf{r}_j} \mathbf{S}_j \right]^2 \right\rangle, \quad (4)$$

where $\mathbf{Q} = (\pi, \pi)$ and \mathbf{S}_j is the electronic spin operator on site j at position \mathbf{r}_j . In contrast to the behavior of the magnons, the fermions-to-pairs ratio does not change considerably at moderate values of t' . Note that at $t' = 0$ all the holes appear as single fermions. This is a manifestation of the absence of pair-binding on the single plaquette at $U = 8t$.

We have found that the same behavior, both in terms of energetics and structure of the ground state, persists

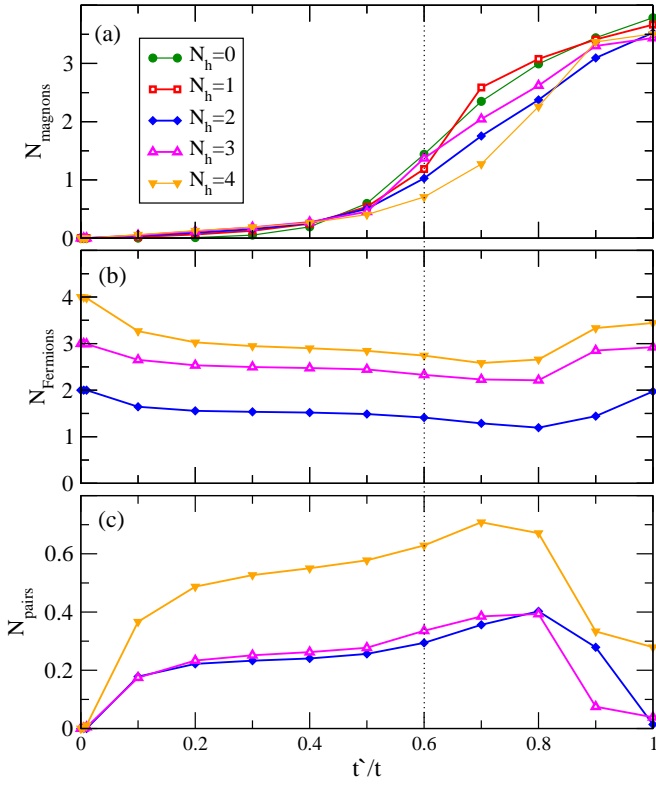


FIG. 9: The average number of (a) magnons, (b) fermions, and (c) hole pairs in the ground state of the 6×6 periodic cluster at $U = 8t$. The position of the pair-binding energy maximum is indicated by the dotted line.

across the entire range of geometries and doping levels which we have studied. Therefore, we conclude that the initial rise of the pair-binding energy for $t' < t'_{\max}$ is kinetic-energy driven. In this range most of the plaquettes are in their half-filled, RVB-correlated ground-state. This type of background facilitates the motion of bound pairs as compared to single holes. When t' approaches t'_{\max} the undoped background changes its nature and becomes more AFM. The gain in kinetic energy associated with hole-pairing saturates and instead a gain in the potential energy of unpaired holes sets in due to their interactions with the AFM magnons. This leads to the decrease of the pair-binding energy.

Another correlation that we were able to establish is between the maximum of the pair-binding energy and the position of the single-hole ground state in momentum space. In both the 4×4 and 6×6 periodic clusters the ground state shifts from the Γ -M and symmetry related directions of the Brillouin-zone to the zone-diagonals as t' is increased through t'_{\max} , see Figs. 2 and 5. Specifically, exact diagonalization¹⁴ of the 4×4 cluster shows that the crystal momentum changes from $(0, \pi)$ and $(\pi, 0)$ to $(0, 0)$ and (π, π) [CORE finds a similar transition to (π, π) but misses the $(0, 0)$ state.] In the 6×6 cluster the shift is from $(0, \pm 2\pi/3)$ and $(\pm 2\pi/3, 0)$ to $(\pm 2\pi/3, \pm 2\pi/3)$ [except for $U = 1 - 3t$ where in a narrow region above t'_{\max}

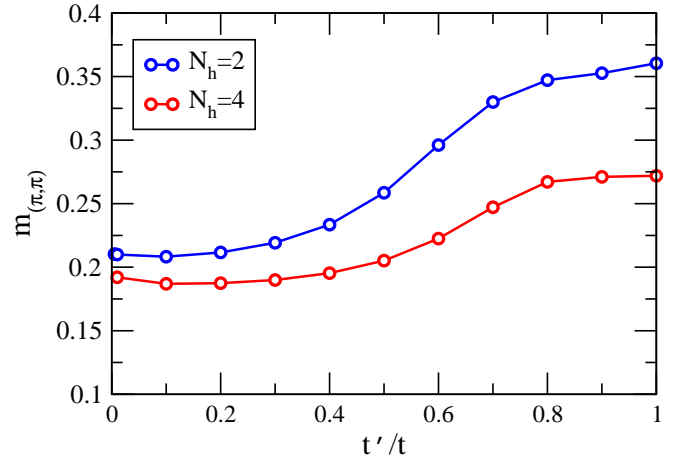


FIG. 10: The staggered magnetization in the two-hole and four-hole ground states of the 6×6 periodic cluster at $U = 8t$.

the ground state is at $(0, 0)$.]

It is known from quantum Monte-Carlo simulations that the single-hole ground state of the *homogeneous* two-dimensional $t - J$ model resides at $(\pm\pi/2, \pm\pi/2)$.¹⁵ One may speculate whether this state is adiabatically connected to the ground state of the inhomogeneous model for $t' > t_{\max}$. The answer to this question is beyond the present study as it requires the diagonalization of larger clusters and the addition of higher-energy plaquette fermions with plaquette momentum $(0, 0)$ and (π, π) to the effective Hilbert space. Regardless of this point, it seems that the transition in the ground state momentum is a possible consequence of the maximum in Δ_{pb} rather than its cause. We arrive at this conclusion based on the fact that in the 4×4 cluster $\Delta_{pb}(3/16)$ exhibits a maximum of similar magnitude to that of $\Delta_{pb}(1/16)$ while the 3-hole ground state is located at $(0, 0)$ and (π, π) over the entire parameter range.¹⁴ In the 6×6 cluster, on the other hand, the maximum in $\Delta_{pb}(3/36)$ is accompanied by a change in the 3-hole ground state momentum, as depicted in Fig. 5.

C. Phase stiffness

In the thermodynamic limit of a d -wave superconductor the pair-binding energy vanishes as $\Delta_{pb} \sim 2\Delta_0 N^{-1/2}$, where Δ_0 is the maximal value of the superconducting gap.⁶ In our rather small clusters we can therefore roughly estimate $\Delta_0 \approx \Delta_{pb}/2$, which together with the d -wave BCS gap relation $T_c = \Delta_0/2.14$, gives

$$T_p = \frac{\Delta_{pb}}{4}, \quad (5)$$

as a characteristic temperature at which pairs fall apart.

The actual T_c may be smaller than T_p if phase fluctuations are important. To obtain an estimate for the phase-ordering temperature T_θ we calculate the ground-

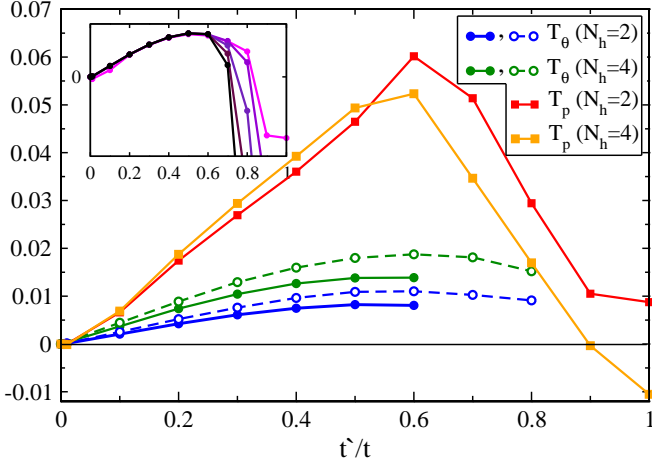


FIG. 11: The pairing scale T_p and the phase coherence scale T_θ in the two-hole and four-hole ground states of the 6×6 periodic cluster at $U = 8t$. T_θ is shown for the cases where the phase twist is introduced at the bond level (solid lines) and at the plaquette level (dashed lines). The inset depicts T_θ of the two-hole system as the phase twist per bond ϕ is varied from $\pi/9$ (upper curve) to $\pi/72$ (lower curve).

state phase stiffness defines as

$$\rho_s = \frac{1}{A} \frac{\partial^2 E}{\partial \phi^2} \bigg|_{\phi=0}. \quad (6)$$

Here E/A is the ground-state energy per unit area and ϕ is a phase twist per bond in the x direction.¹⁶ Neglecting the suppression of the stiffness due to thermal excitation of gapless nodal quasiparticles and using the relation $T_c = 0.89\rho_s$ for the two-dimensional XY model we obtain the estimator

$$T_\theta = \rho_s. \quad (7)$$

We have calculated ρ_s in two ways. In the first the phase twist was introduced into the Hamiltonian (1) by changing $t_{ij} \rightarrow t_{ij}e^{i\phi/2}$ for two nearest-neighbor sites in the x direction. The effective CORE Hamiltonian for the twisted system was then derived and diagonalized to obtain the ϕ dependence of the ground state energy. In the second way the twist was introduced on the plaquette level by modifying the couplings in the effective CORE Hamiltonian for the untwisted model (1). This was achieved via multiplication of a coupling between two neighboring plaquettes in the x direction that changes the number of holes on the right plaquette by Δn , by $e^{i\phi\Delta n}$.

The phase-ordering temperature of the periodic 6×6 cluster with two and four holes is depicted in Fig. 11. The two methods yield similar results and they both encounter problems in the region $t' > t'_{\max}$. The nature of the difficulty is demonstrated by the inset of Fig. 11, showing ρ_s as calculated from a discrete derivative of the ground state energy with respect to a twist introduced at the bond level. When the derivative is calculated for

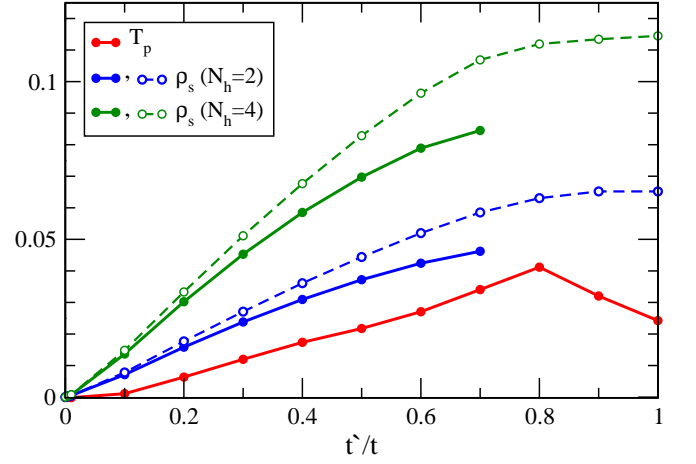


FIG. 12: The pairing scale T_p and the phase stiffness of a 14×2 ladder in the two-hole and four-hole ground states at $U = 8t$. T_p is essentially the same for the two hole doping levels. The solid (dashed) ρ_s lines were calculated by introducing the phase twist at the bond (plaquette) level.

increasingly smaller values of ϕ the result does not converge for $t' > t'_{\max}$. Rather, it becomes negative and diverges, indicating that the CORE ground-state energy develops a cusp as function of ϕ . A similar behavior is also found in the 4×4 periodic cluster and in the ladder systems. It occurs at lower values of t' for systems with odd number of holes. We take these findings as an indication that CORE is unable to produce a reliable approximation for ρ_s in the region beyond the maximum in the pairing scale.

In the range $t' < t'_{\max}$ the estimated phase-ordering temperature increases monotonically with t' , but is consistently below the pairing scale. At $t' = t'_{\max}$ we find for the two-hole system $T_p/T_\theta \approx 6$. Increasing the doping to four holes decreases the maximal T_p slightly and increases T_θ by about 70% leading to $T_p/T_\theta(t' = t'_{\max}) \approx 3$. The same holds true for the 4×4 cluster with two holes, which has a similar hole density and $T_p/T_\theta(t' = t'_{\max}) \approx 2$. Such a behavior suggests that superconductivity in the lightly doped two-dimensional checkerboard Hubbard model is governed by phase fluctuations. In ladders our definition Eq. (6) is equivalent to the phase stiffness along the ladder ($v_c K_c$ in the effective Luttinger liquid description of the system) divided by its width. As shown by Fig. 12 it is larger than the corresponding stiffness in the periodic clusters and grows with doping. However, since the one-dimensional system can not order it does not provide a phase ordering temperature similar to Eq. (7).

D. Pairing correlations

Another diagnostic tool for the presence of superconductivity is the pair-field correlation function. We have

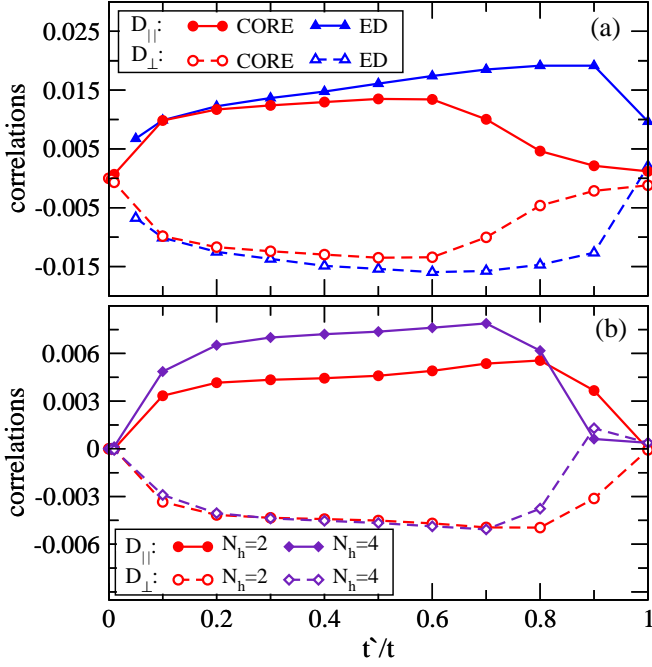


FIG. 13: Pair-field correlations at $U = 8t$ in the ground state of (a) the 2-hole doped 4×4 periodic cluster, including a comparison to the exact results of Ref. 6, and (b) the 2-hole and 4-hole doped 6×6 periodic cluster. D_{\perp} and D_{\parallel} are the correlations between the pair-field on bond \overline{ab} and the pair field on bonds \overline{cd} and \overline{ef} , respectively, as defined by Fig. 1.

calculated the following equal-time correlator

$$D_{\overline{ij}, \overline{kl}} = \langle \Delta_{ij}^{\dagger} \Delta_{kl} \rangle, \quad (8)$$

where \overline{ij} denotes the bond between the nearest-neighbor sites i and j , and where the pair field on that bond is given by

$$\Delta_{ij}^{\dagger} = \frac{1}{\sqrt{2}}(c_{i\uparrow}^{\dagger}c_{j\downarrow}^{\dagger} + c_{j\uparrow}^{\dagger}c_{i\downarrow}^{\dagger}). \quad (9)$$

Fig. 13 shows the results for the pair-field correlations between the two most distant parallel (D_{\parallel}) and perpendicular (D_{\perp}) bonds on the periodic clusters with $N_h = 2$ and $N_h = 4$. Similar results were also obtained for the ladder systems. We find that D_{\parallel} is positive and D_{\perp} is negative, consistent with d -wave pairing. The pairing correlations diminish in the limits $t'/t \rightarrow 0$ and $t'/t \rightarrow 1$ but unlike the pair-binding energy and the phase stiffness they are nearly independent of t' in the range of moderate inhomogeneity (from $t' = 0.1t$ to $t' = 0.6t$ Δ_{pb}, ρ_s and D change by a factor of 7.5, 4.5, and 1.5, respectively.) The magnitude of the correlations is small and comparable to results of previous studies of Hubbard ladders¹⁷ and Hubbard² and $t - J$ periodic clusters.¹⁸

The behavior of D suggests that pairing is very weak in the systems that were studied. This conclusion is in apparent contradiction with the large pair-binding energy found in the same clusters. In addition, as we already

noted, the t' -dependence of the two quantities is very different. We believe that the fault may lie in the specific form of the pair-field, Eq. (9), that was used for calculating the pairing correlations. It assumes a pair-wavefunction which is strongly localized in space. This may be wrong, as suggested by our results for the structure of the ground-state. Fig. 9 clearly shows that most holes are not bound into pairs on a single plaquette. This is expected since for $U = 8t$ the plaquette does not provide a positive pair-binding energy. It seems, therefore, that thinking about Cooper-pairing in such systems in terms of real-space pairs occupying single bonds is a misleading oversimplification. Most likely, the phenomenon is more complicated and the pair wavefunction, while being much more localized than its counterpart in conventional superconductors, still possesses a non-trivial real-space structure.

IV. CONCLUSIONS

This study had a dual motivation. First, to explore the utility of the CORE approximation as a method to investigate fermionic strongly correlated systems, and secondly to shed additional light on the role of inhomogeneity in the physics of high-temperature superconductivity.

As far as CORE is concerned, it is difficult to carry out the original scheme of Morningstar and Weinstein⁸ who iteratively applied the CORE method to obtain and analyze a fixed point Hamiltonian. In the case of the Hubbard model there are simply too many couplings that are generated at each step. One is, therefore, forced to apply CORE once and investigate the resulting effective Hamiltonian either by means of a mean-field approximation⁹, or via numerical diagonalization of finite clusters. The latter approach was previously implemented in the study of spin systems^{19,20} and the $t - J$ model^{10,11}, and is the one which we pursued. As expected, when applied to the checkerboard Hubbard model range-2 CORE provides results which are in good agreement with the available exact diagonalization results in the limit of small t' . In the moderate t' regime the method may be considered as semiquantitative and its validity in the uniform limit is questionable, particularly in the case of small U . More precisely, this statement depends on the property that one tries to calculate using the method. It seems that pairing is moderately local such that range-2 CORE is able to capture its salient features already in small systems. The establishment of phase coherence, on the other hand, is a more extended phenomenon, for which the inclusion of longer range effective interactions and diagonalization of larger clusters are needed. In this context we would like to note that signatures associated with nodal quasiparticles of the putative d -wave Hubbard superconductor, such as the suppression of the phase stiffness at low temperatures, are particularly difficult to capture using range-2 CORE.⁹

Regarding the effects of inhomogeneity, our results

demonstrate that plaquettization of the Hubbard model may lead to a substantial enhancement of pairing. Optimal pairing is achieved at an intermediate scale of inhomogeneity, which marks a crossover from a region with pronounced RVB characteristics to one with stronger local AFM correlations. The interactions of the doped holes with the spin background are the driving force of the pairing process. One should bare in mind, however, that the Hubbard plaquette, the building block of our model, is a special system. Its undoped ground state is a quintessential RVB state and it provides a positive pair-binding energy in a wide range of interaction strengths. Hence, it is interesting to ask whether a similar enhancement occurs for other plane patterns, especially those constructed from elementary clusters that do not exhibit pair binding. The possibility of such an outcome gains support from the fact that in the checkerboard model maximal pairing occurs at an interaction strength for which the pair-binding energy on each individual plaquette is negative.

In the lightly doped clusters that we have studied superconductivity appears to be controlled by phase fluctuations. Owing to the reasons outlined above and our inability to carry out significant finite-size scaling it is difficult to estimate the phase ordering temperature in the two-dimensional limit and determine whether T_c indeed achieves a maximum at an intermediate value of t' . T_c enhancement due to inhomogeneous pairing interaction was found in the attractive Hubbard model^{21–25} and the phase-ordering transition temperature is raised in the classical two-dimensional XY model with certain "framework" modulations of the phase couplings.²⁶ We find it interesting to conclude by noting that Fig. 11 hints at the possibility that a related inhomogeneity-induced enhancement occurs in the model considered here as well.

Acknowledgments

We are most grateful to the authors of Ref. 6, in particular to Wei-Feng Tsai, for providing us with the results of the exact diagonalization of the 4×4 Hubbard cluster. It is also our pleasure to thank Sylvain Capponi for his valuable help in verifying our CORE calculations, and Erez Berg for stimulating discussions. This work was supported by the Israel Science Foundation (grants No. 538/08 and 459/09) and by the United States - Israel Binational Science Foundation (grant No. 2008085).

Appendix A: The CORE Hamiltonian

The full CORE Hamiltonian includes all possible terms that satisfy the symmetries of the problem, as detailed in Section II. The resulting 45 effective couplings may be grouped in the following way

$$H = K_{bf} + K_{bf+t} + V_{bf} + V_t. \quad (\text{A1})$$

The kinetic energy of the fermionic holes and the bosonic pairs is given by the first two terms. K_{bf} contains the contribution of hopping processes involving only the charged degrees of freedom while K_{bf+t} contains similar processes in which the triplet of AFM magnons also participate. The interactions among the fermions and pairs comprise V_{bf} . Their remaining interactions with the magnon triplet, as well as couplings involving only the triplets, form the last group V_t .

In the following, b_i^\dagger , $t_{\sigma i}^\dagger$ and $f_{\mathbf{q}\sigma i}^\dagger$ create a hole pair, a magnon with spin component $S_z = \sigma$ and a fermion with spin component $S_z = \sigma$ and plaquette momentum \mathbf{q} at site i , respectively. Our choice to use a basis where the two fermions have a definite plaquette momentum $\mathbf{q} = (0, \pi)$ or $\mathbf{q} = (\pi, 0)$ results in different interaction strengths between nearest neighbors in the x direction compared to the y direction. The notation $\langle i, j \rangle_\nu$ in the Hamiltonian below stands for nearest neighbors in the $\nu = x, y$ direction and $(A_i B_j)_{S, \sigma}$ signifies that the operators A_i and B_j are coupled into an operator of total spin S and spin component $S_z = \sigma$. Finally, summation over S, σ, \mathbf{q} , and ν indices is implied.

The 7 "bare" kinetic couplings include fermion and pair hopping, as well as pair-fermion exchange and Andreev-like pair creation and disintegration.

$$\begin{aligned} K_{bf} = & J_b \sum_{\langle i, j \rangle} b_i^\dagger b_j \\ & + J_f^{\nu, \mathbf{q}} \sum_{\langle i, j \rangle_\nu} f_{\mathbf{q}\sigma i}^\dagger f_{\mathbf{q}\sigma j} \\ & + J_{bf}^{\nu, \mathbf{q}} \sum_{\langle i, j \rangle_\nu} b_i^\dagger f_{\mathbf{q}\sigma j}^\dagger b_j f_{\mathbf{q}\sigma i} \\ & + J_{bff}^{\nu, \mathbf{q}} \sum_{\langle i, j \rangle_\nu} \left[b_i^\dagger f_{\mathbf{q}\uparrow i} f_{\mathbf{q}\downarrow j} + b_i^\dagger f_{\mathbf{q}\uparrow j} f_{\mathbf{q}\downarrow i} + \text{H.c.} \right]. \quad (\text{A2}) \end{aligned}$$

Note that since the Hamiltonian is symmetric under rotations and reflections some of the couplings are related. For example, $J_f^{x, \mathbf{q}} = J_f^{y, \bar{\mathbf{q}}}$, where $\bar{\mathbf{q}} = \mathbf{q} + (\pi, \pi) \bmod 2\pi$. These symmetries and the d -wave symmetry of the plaquette hole-pair state also imply $J_{bff}^{x, \mathbf{q}} = -J_{bff}^{y, \bar{\mathbf{q}}}$.

The remaining 9 kinetic couplings are associated with magnon-assisted hopping processes

$$\begin{aligned} K_{bf+t} = & J_{bt} \sum_{\langle i, j \rangle} b_i^\dagger t_{\sigma j}^\dagger b_j t_{\sigma i} \\ & + J_{ft}^{S, \nu, \mathbf{q}} \sum_{\langle i, j \rangle_\nu} (t_i^\dagger f_{\mathbf{q}j}^\dagger)_{S, \sigma} (t_j f_{\mathbf{q}i})_{S, \sigma} \\ & + J_{fft}^{\nu, \mathbf{q}} \sum_{\langle i, j \rangle_\nu} \left[(t_i^\dagger f_{\mathbf{q}j}^\dagger)_{\frac{1}{2}, \sigma} f_{\bar{\mathbf{q}}\sigma i} + \text{H.c.} \right] \\ & + J_{bft}^{\nu, \mathbf{q}} \sum_{\langle i, j \rangle_\nu} \left[b_i^\dagger t_{\sigma j}^\dagger (f_{\mathbf{q}i} f_{\bar{\mathbf{q}}j})_{1, \sigma} + \text{H.c.} \right]. \quad (\text{A3}) \end{aligned}$$

The 16 fermion and pair on-site energies and interac-

tions are

$$\begin{aligned}
V_{bf} = & \epsilon_{f\mathbf{q}} \sum_i f_{\mathbf{q}i}^\dagger f_{\mathbf{q}\sigma i} + \epsilon_b \sum_i b_i^\dagger b_i \\
& + V_b \sum_{\langle i,j \rangle} b_i^\dagger b_j^\dagger b_j b_i + V_{bf}^{\nu,\mathbf{q}} \sum_{\langle i,j \rangle_\nu} b_i^\dagger f_{\mathbf{q}\sigma j}^\dagger f_{\mathbf{q}\sigma j} b_i \\
& + V1_{ff}^{S,\nu,\mathbf{q}} \sum_{\langle i,j \rangle_\nu} (f_{\mathbf{q}j}^\dagger f_{\mathbf{q}i}^\dagger)_{S,\sigma} (f_{\mathbf{q}i} f_{\mathbf{q}j})_{S,\sigma} \\
& + V2_{ff}^S \sum_{\langle i,j \rangle_\nu} (f_{\mathbf{q}j}^\dagger f_{\mathbf{q}i}^\dagger)_{S,\sigma} (f_{\bar{\mathbf{q}}i} f_{\bar{\mathbf{q}}j})_{S,\sigma} \\
& + V3_{ff}^S \sum_{\langle i,j \rangle_\nu} (f_{\mathbf{q}j}^\dagger f_{\bar{\mathbf{q}}i}^\dagger)_{S,\sigma} (f_{\mathbf{q}i} f_{\bar{\mathbf{q}}j})_{S,\sigma} \\
& + V4_{ff}^S \sum_{\langle i,j \rangle_\nu} (f_{\mathbf{q}j}^\dagger f_{\bar{\mathbf{q}}i}^\dagger)_{S,\sigma} (f_{\bar{\mathbf{q}}i} f_{\mathbf{q}j})_{S,\sigma}. \quad (\text{A4})
\end{aligned}$$

The fermion on-site energies depend on \mathbf{q} in ladders where the symmetry between the x and y directions is broken. The on-site energies on a plaquette depend on the number of its nearest neighbors. Therefore, they may be position dependent in finite clusters without periodic boundary conditions. This does not happen for the clus-

ters that we have investigated.

The last group consists of 13 couplings involving the magnons. They include their on-site energy, excitation amplitude from the vacuum, hopping matrix element and the strength of their mutual interaction together with their interaction couplings to the fermions and bosons. We find the coupling to the bosons to be very small.

$$\begin{aligned}
V_t = & \epsilon_t \sum_i t_{\sigma i}^\dagger t_{\sigma i} + J_{tt} \sum_{\langle i,j \rangle} \left[(t_i^\dagger t_j^\dagger)_0 + \text{H.c.} \right] \\
& + J_t \sum_{\langle i,j \rangle} t_{\sigma i}^\dagger t_{\sigma j} + V_{tt}^S \sum_{\langle i,j \rangle} (t_i^\dagger t_j^\dagger)_{S,\sigma} (t_j t_i)_{S,\sigma} \\
& + V_{bt} \sum_{\langle i,j \rangle} b_i^\dagger t_{\sigma j}^\dagger t_{\sigma j} b_i \\
& + V_{ft}^{S,\nu,\mathbf{q}} \sum_{\langle i,j \rangle_\nu} (t_i^\dagger f_{\mathbf{q}j}^\dagger)_{S,\sigma} (f_{\mathbf{q}j} t_i)_{S,\sigma} \\
& + V_{ft}^{\nu,\mathbf{q}} \sum_{\langle i,j \rangle_\nu} \left[(t_i^\dagger f_{\mathbf{q}j}^\dagger)_{\frac{1}{2},\sigma} f_{\bar{\mathbf{q}}\sigma j} + \text{H.c.} \right]. \quad (\text{A5})
\end{aligned}$$

-
- ¹ For a review see E. W. Carlson, V. J. Emery, S. A. Kivelson, and D. Orgad, in *"Superconductivity: Novel Superconductors"*, Vol 2, p. 1225, edited by K. H. Bennemann and J. B. Ketterson (Springer-Verlag 2008).
- ² T. Aimi and M. Imada, J. Phys. Soc. Jpn. **76**, 113708 (2007).
- ³ E. Arrigoni and S. A. Kivelson, Phys. Rev. B **68**, 180503(R) (2003).
- ⁴ E. Arrigoni, E. Fradkin, and S. A. Kivelson, Phys. Rev. B **69**, 214519 (2004).
- ⁵ W.-F. Tsai and S. A. Kivelson, Phys. Rev. B **73**, 214510 (2006), *ibid* **76**, 139902 (2007).
- ⁶ W.-F. Tsai, H. Yao, A. Läuchli, and S. A. Kivelson, Phys. Rev. B **77**, 214502 (2008).
- ⁷ D. G. S. P. Doluweera, A. Macridin, T. A. Maier, M. Jarrell, and Th. Pruschke, Phys. Rev. B **78**, 020504(R) (2008).
- ⁸ C. J. Morningstar and M. Weinstein, Phys. Rev. D **54**, 4131 (1996).
- ⁹ E. Altman and A. Auerbach, Phys. Rev. B **65**, 104508 (2002).
- ¹⁰ D. Poilblanc, E. Orignac, S. R. White, and S. Capponi, Phys. Rev. B **69**, 220406(R) (2004).
- ¹¹ S. Capponi and D. Poilblanc, Phys. Rev. B **66**, 180503 (2002).
- ¹² C. S. Hellberg and E. Manousakis, Phys. Rev. Lett. **78**, 4609 (1997).
- ¹³ D. Poilblanc, O. Chiappa, J. Riera, S. R. White, and D. J. Scalapino, Phys. Rev. B **62**, R14633 (2000).
- ¹⁴ W.-F. Tsai (private communication).
- ¹⁵ M. Brunner, F. F. Assaad, and A. Muramatsu, Phys. Rev. B **62**, 15480 (2000).
- ¹⁶ D. J. Scalapino, S. R. White, and S. Zhang, Phys. Rev. B **47**, 7795 (1993).
- ¹⁷ R. M. Noack, S. R. White, and D. J. Scalapino, Phys. Rev. Lett. **73**, 882 (1994).
- ¹⁸ S. Sorella, G. B. Martins, F. Becca, C. Gazza, L. Capriotti, A. Parola, and E. Dagotto, Phys. Rev. Lett. **88**, 117002 (2002).
- ¹⁹ J. Piekarewicz and J. R. Shepard, Phys. Rev. B **57**, 10260 (1998).
- ²⁰ S. Capponi, A. Läuchli, and M. Mambrini, Phys. Rev. B **70**, 104424 (2004).
- ²¹ I. Martin, D. Podolsky, and S. A. Kivelson, Phys. Rev. B **72**, 060502(R) (2005).
- ²² K. Aryanpour, E. R. Dagotto, M. Mayr, T. Paiva, W. E. Pickett, and R. T. Scalettar, Phys. Rev. B **73**, 104518 (2006).
- ²³ K. Aryanpour, T. Paiva, W. E. Pickett, and R. T. Scalettar, Phys. Rev. B **76**, 184521 (2007).
- ²⁴ Y. Zou, I. Klich, and G. Refael, Phys. Rev. B **77**, 144523 (2008).
- ²⁵ V. Mishra, P. J. Hirschfeld, and Y. S. Barash, Phys. Rev. B **78**, 134525 (2008).
- ²⁶ Y. L. Loh and E. W. Carlson, Phys. Rev. B **75**, 132506 (2007).